PHOTOMASK

BACUS—The international technical group of SPIE dedicated to the advancement of photomask technology.

Photomask Japan 2012
Best Poster Award

Shedding Light on EUV Mask Inspection

Kazunori Seki and Toshio Konishi, Toppan Photomasks Inc, 1000 River St., Essex Junction, VT 05452, USA

Karen Badger and Emily Gallagher, IBM Microelectronics, 1000 River St., Essex Junction, VT 05452, USA

Gregory McIntyre, IBM Microelectronics, 257 Fuller Road, Albany, NY 12203, USA

ABSTRACT

EUV defect detectability is evaluated both through simulation and by conventional mask inspection tools at various wavelengths (13.5, 193, 257, 365, 488 and 532 nm). The simulations reveal that longer wavelength light penetrates deeper into the multilayer than shorter wavelength light, however this additional penetration does not necessarily provide an advantage over shorter wavelengths for detecting defects. Interestingly, for both blank and patterned mask inspections, each wavelength detected unique defects not seen at other wavelengths. In addition, it was confirmed that some of the defects that are detected only by longer wavelengths are printable. This study suggests that a combination of wavelengths may be the most comprehensive approach to finding printable defects as long as actinic inspection is not available.

1. Introduction

EUV (*Extreme Ultraviolet*) lithography is one of the most promising techniques for imaging 10-nm node wafer features. There are several challenges associated with moving EUV lithography from development to manufacturing and mask defectivity is one of the largest. EUV mask inspection may require more advanced approaches than those currently employed on optical masks. Where both transmitted and

Continues on page 3.

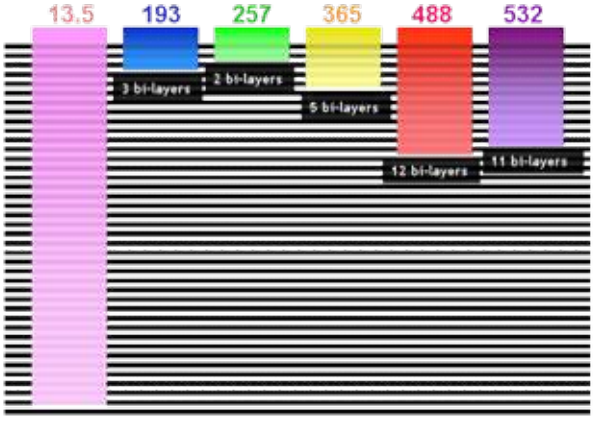

Figure 1. Light penetration into Mo/Si multilayer at multiple wavelengths.

BACUS NEWS
SEPTEMBER 2012
VOLUME 28, ISSUE 9

TAKE A LOOK INSIDE:

SPIE

EDITORIAL

Open Possibilities

Jon Haines, Micron Technology, Inc.

When it comes to spring cleaning, removing excess heat is not a commonly listed activity. So I guess my list this past spring was a bit uncommon when I consciously decided it was time to evict my old P4 desktop computer. The large desktop box, affectionately named "space-heater" by my wife, has graciously devolved over the years into a file server devoted to home videos, pictures, and the occasional printout.

After a bit of research on the Web, I zeroed in on the idea of replacing the space heater with a network-attached hard drive. Unfortunately, the compact versions that caught my eye had already been earning a "poor" or "limited" software reputation among many online critics. Fortunately, for my needs, some models were running with an open-source operating system. After a few clicks, patience with the domestic mail system, and support from my online Linux entourage, I confidently swapped out the software on one of the open-source units for something much more obedient. With the original manufacturer's software retired to an archived folder, a new suite of open-source programs shouldered the task of serving up videos, pictures, and remote peripheral needs to my family's domesticated network gadgets. In a way, it is a bit comical to see a stapler-sized box, originally destined to be only a file server, being itself serviced by the surrounding team of USB-connected scanner, printers, and external hard drives.

So what does this weekend project have to do with photomasks? Well, if we are talking about improving photomasks and improving things that improve them… quite a lot! Just like the aforementioned consumer products (coincidently made possible with the use of photomasks), photomasks have also benefited from similar "open" initiatives.

I would like to preemptively dispel the idea that I am making any comparison about the quality or performance of currently available software. The vast majority of commercial software packages used in the manufacturing of photomasks continues to be at the forefront of the craft. That being said, for at least the last decade I have witnessed an ever-increasing number of photomask-equipment vendors offering one form or another of open- content. The most prevalent forms advertised are human-readable scripts, recipes, and output files (e.g. editable text, XML, etc.) as well as source-code utilizing proprietary programming libraries (e.g. C/C++ DLL, Java, etc.).

Following essentially the same philosophy as open-source, open-content promotes end-user development of additional capabilities without the expectation of vendor ownership or control over technological derivatives. Many of the arguments used for and against open-content mirror arguments supporting and opposing open-source. Two of the most common areas of contention have been technology sharing and vendor profitability.

Open-content critics might argue that open-content options lead to greater photomask technology disparity between manufacturers. Technologies derived with open-content can be developed independently allowing them to be closely held by the creator, thereby depriving the industry of the capability and fostering isolation. Without open-content, a manufacturer is encouraged (or forced) to develop new technology with the software-vendor as a team, eventually extending the capability to other manufacturers via future software releases.

However, while agreeing with the isolating risks of open-content, I would argue that this risk is not the significant factor in determining the amount of technology shared. Behind the premise that open-content is a technology isolator is the assumption that there is little to be gained by sharing technological advantages with competitors. Short of writing a second editorial on the subject of IP sharing, I will simply put forth the fact that there are often multiple business and market advantages to sharing and developing technology across the industry. Because some percentage of new technology will always be shared, the total shared amount is more likely driven by the rate of technology creation.

Utilizing open-content increases the rate at which new technologies are discovered, thereby increasing the amount of technologies that could be potentially shared. For example, the development resources of a single photomask-equipment vendor are small in comparison to the combined resources of all photomask manufacturers. It is unlikely that a vendor could investigate every sharable idea created by all photomask

(continues on page 11)

BACUS

N • E • W • S

BACUS News is published monthly by SPIE for BACUS, the international technical group of SPIE dedicated to the advancement of photomask technology.

Managing Editor/Graphics Linda DeLano

Advertising Lara Miles

BACUS Technical Group Manager Pat Wight

■ 2012 BACUS Steering Committee ■

President
Wolfgang Staud, *Applied Materials, Inc.*

Vice-President
John Whittey, *KLA-Tencor MIE Div.*

Secretary
Artur Balasinski, *Cypress Semiconductor Corp.*

Newsletter Editor
Artur Balasinski, *Cypress Semiconductor Corp.*

2012 Annual Photomask Conference Chairs
Frank E. Abboud, *Intel Corp.*
Thomas B. Faure, *IBM Corp.*

International Chair
Naoya Hayashi, *Dai Nippon Printing Co., Ltd.*

Education Chair
Artur Balasinski, *Cypress Semiconductor Corp.*

Members at Large
Paul W. Ackmann, *GLOBALFOUNDRIES Inc.*
Michael D. Archuletta, *RAVE LLC*
Uwe Behringer, *UBC Microelectronics*
Peter D. Buck, *Toppan Photomasks, Inc.*
Brian Cha, *Samsung*
Kevin Cummings, *ASML US, Inc.*
Glenn R. Dickey, *Shin-Etsu MicroSi, Inc.*
Thomas B. Faure, *IBM Corp.*
Brian J. Grenon, *Grenon Consulting*
Jon Haines, *Micron Technology Inc.*
Mark T. Jee, *HOYA Corp, USA*
Bryan S. Kasprowicz, *Photronics, Inc.*
Oliver Kienzle, *Carl Zeiss SMS GmbH*
Wilhelm Maurer, *Infineon Technologies AG*
M. Warren Montgomery, *The College of Nanoscale Science and Engineering (CNSE)*
Abbas Rastegar, *SEMATECH North*
Emmanuel Rausa, *Plasma-Therm LLC.*
Douglas J. Resnick, *Molecular Imprints, Inc.*
Steffen F. Schulze, *Mentor Graphics Corp.*
Jacek K. Tyminski, *Nikon Precision Inc.*
Larry S. Zurbrick, *Agilent Technologies, Inc.*

SPIE

P.O. Box 10, Bellingham, WA 98227-0010 USA
Tel: +1 360 676 3290
Fax: +1 360 647 1445
SPIE.org
help@spie.org

©2012

All rights reserved.

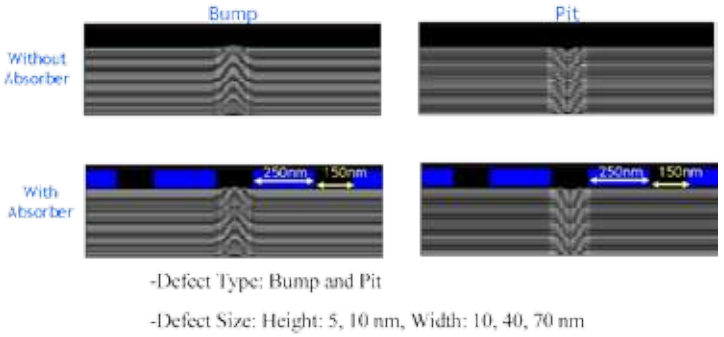

Figure 2. Sample defect images of bumps and pits.

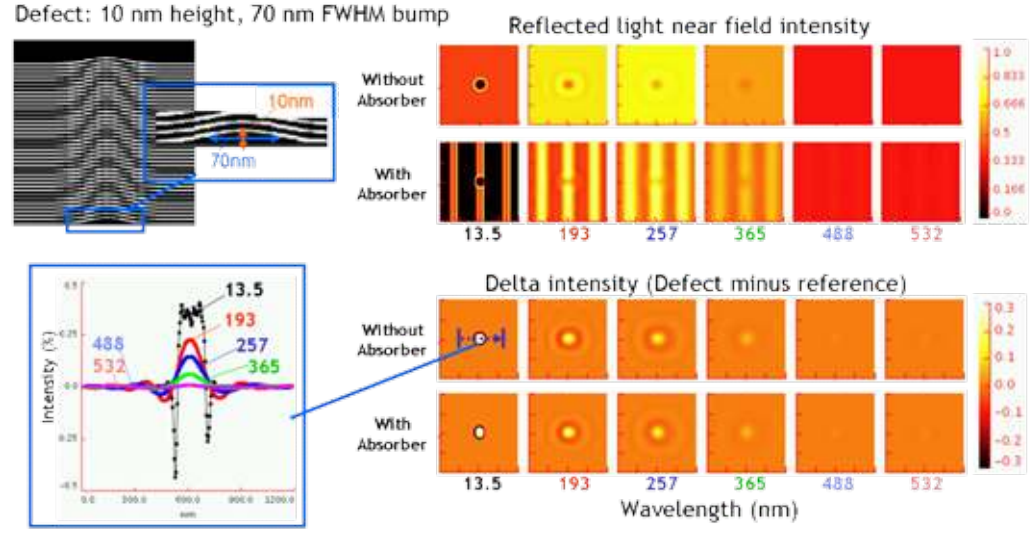

Figure 3. Defect images are shown with and without patterned absorber at various wavelengths.

reflected light are used for optical mask inspection, only reflected light is available for EUV because the masks are reflective.[1] EUV blanks consist of many layers: LTEM (Low Thermal Expansion Material) substrate, backside conductive layer, front side reflective stack of 40 to 50 of Mo/Si bilayers, a Ru protective cap, and the Ta-based absorber material. Mask inspection must detect not only film surface defects but also bilayer and backside defects. At the same time, the minimum defect size continues to shrink; according to the ITRS road map, the defect criteria will be 25 nm in 2012 and 18 nm in 2015.

Historically, newer generation inspection tools deploy shorter wavelengths to improve inspectability and improve the defect detection sensitivity. For EUV masks, none of the standard inspection wavelengths will penetrate the reflective multilayers. Only the actinic inspection wavelength of 13.5 nm will be capable of detecting all the relevant defects. Unfortunately, actinic EUV mask inspection will not be available for at least three years. During the interim, all available methods of detecting and characterizing defects that matter must be deployed.[2] Since defects can exhibit wavelength-dependent characteristics, it is possible that selecting non-standard inspection wavelengths may provide an advantage. This paper will compare EUV mask inspection results at 193, 257, 365, 488 and 532 nm. An assessment of defect printability at 13.5 nm will be used to determine whether the non-standard wavelengths improve the identification of printable EUV mask defects. An alternate wavelength may add EUV mask detection capability while the industry waits for actinic inspection tools.

2. Experiments

2.1 Simulation study

2.1.1 Light penetration

Light penetration of some wavelengths have already been reported.[3] We executed a similar simulation using a range of available inspection wavelengths including 257, 365 and 532 nm light. A schematic representation of the result is shown in Figure 1. The wavelength used for most advanced mask pattern inspection is 193 nm; it penetrates only 3 bilayers. Clearly that wavelength will miss

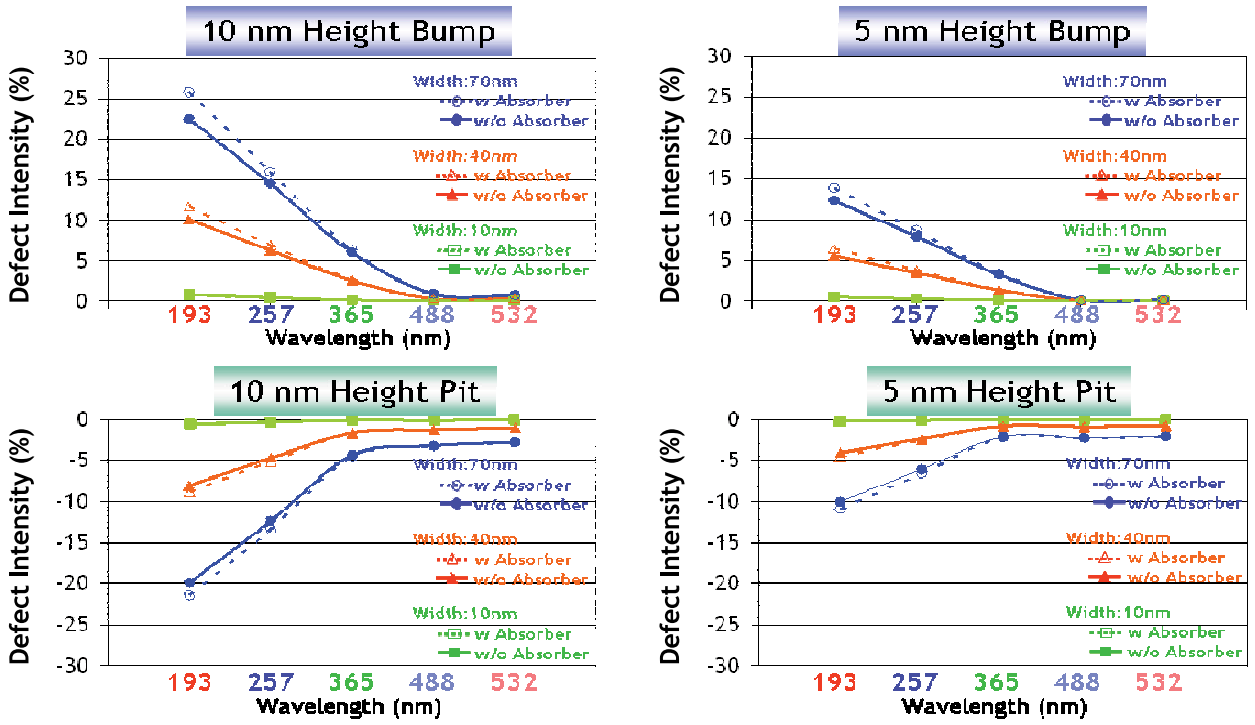

Figure 4. Defect intensity for bumps and pits is compared at various wavelengths.

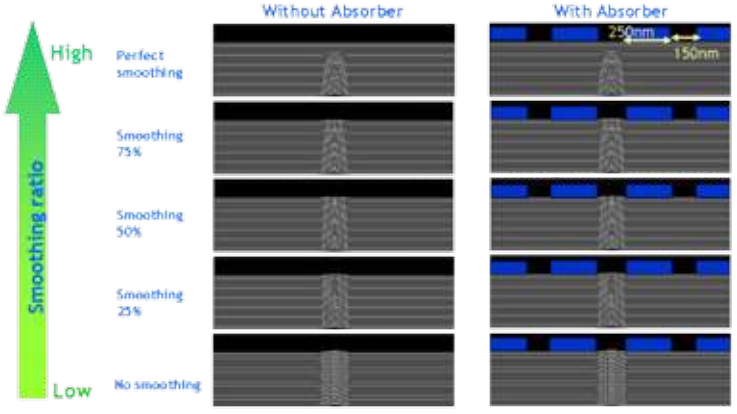

Figure 5. Test schematic images for the smoothing study with and without the absorber pattern.

phase defects that lack any disruption in the top layers of the multilayer stack. Interestingly, 365, 488 and 532 nm wavelengths penetrate deeper into the multilayer than the 193 nm wavelength. The inspection tools associated with the longer wavelengths are mainly used for older technology photomasks because they are associated with older generations of tools that were designed for larger mask patterns. Consequently, they have a lower sensitivity for many defect types. For this study, longer wavelength light may demonstrate better detection capabilities than shorter wavelength light for certain phase defects. It is worth noting that only 13.5 nm actinic inspection is capable of detecting all phase defects because it penetrates so deeply into the multilayer.

2.1.2 Phase defect detectability

Defect detectability of bump and pit defects are compared at various wavelengths. Figure 2 shows a 2D slice through the 3D structure of these Gaussian-shaped multilayer defects. The defect heights studied are 5 and 10 nm and full width half maximum (FWHM) widths are 10, 40, and 70 nm. Rigorous 3D Finite Difference Time Domain (FDTD) simulation was performed to determine the relative detection signal of each defect using the wavelengths from Figure 1. A plane wave was incident on the mask and the

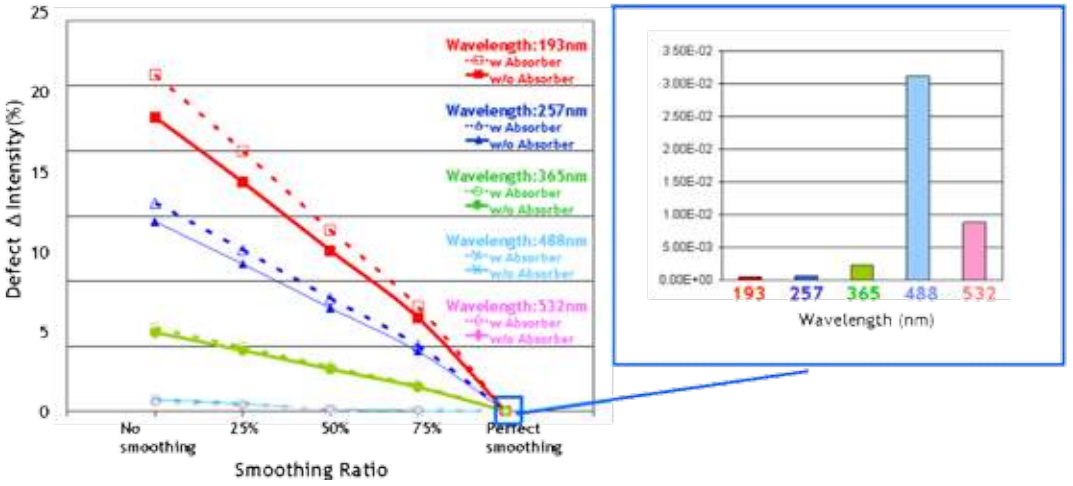

Figure 6. Light intensity comparison result of smoothing defects.

near field light intensity was taken as the output signal. This intensity represents the optimum defect sensitivity since the inherent losses associated with detection are not included. Each defect was simulated both with and without the presence of the absorber pattern.

Figure 3 shows sample simulation results for a 70 nm wide, 10 nm high bump defect illuminated by various wavelengths. To understand the relative detectability of this defect for each wavelength, the near field intensity is studied just after light reflects from the ML surface. This replicates the intensity that a perfect measurement inspection system would see and provides a fair comparison between wavelengths without knowing the proprietary design of any particular commercial inspection system. It is likely that most current inspection systems detect a majority of this signal. The delta intensity images, an example is the lower left series in Figure 3, describe the difference in intensity between the defect and a no-defect reference image, similar to a die-to-die or die-to-model measurement. The peak of this delta intensity is defined as the defect intensity and will be used as the primary metric throughout the remainder of this section. As the delta intensity picture shows, there is no significant intensity difference with and without the absorber. Thus, as long as the defect is located in the center of the open feature, the presence of the absorber has marginal effect on the detectability of the defect. Section 2.1.4 will address what happens when the defect location varies. It is also observed in Figure 3 that longer wavelengths such as 488 nm and 532 nm detect lower intensity than shorter ones and 13.5 nm light shows the highest intensity.

Figure 4 compares the intensity change caused by a defect relative to the no defect case as a function of wavelength. The patterned absorber condition shows slightly higher intensity than the cases without absorber. Shorter wavelengths detect higher intensity than longer ones for both bump and pit defects. Longer wavelengths detect lower intensities for all of the simulated defects. So, depending on the specifics of a given inspection system, it is possible that only 193 nm and 257 nm wavelengths have the potential to detect these bump and pit defects. It is also observed that bumps are slightly more detectable than pits, showing a 10 to 15% greater intensity signal.

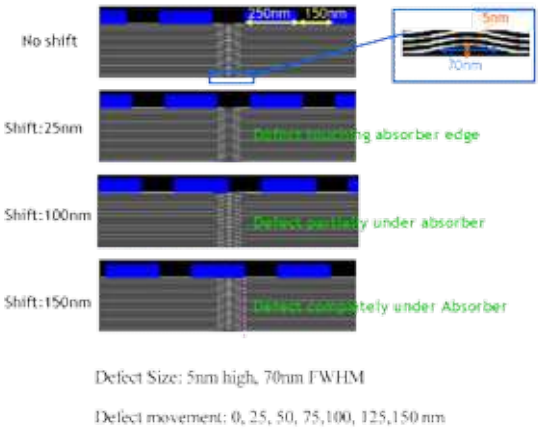

Figure 7. Test sample images of the defect location study.

2.1.3 Smoothing Case study

This section investigates the detectability of multilayer phase defects in the presence of varying degrees of smoothing during the multilayer deposition process. Previous studies have shown that sometimes programmed multilayer defects show different inspectability, detectability and wafer printability compared with native defects.[4,5] Here, natural-like programmed defects are simulated and evaluated using smoothing. The smoothing ratio denotes the peak of the Gaussian at the top of the multilayer relative to that at the bottom, with the peak varying linearly in between. In the case of perfect smoothing, there is no defect topography on film surface. Conditions with and without the absorber pattern are compared in Figure 5.

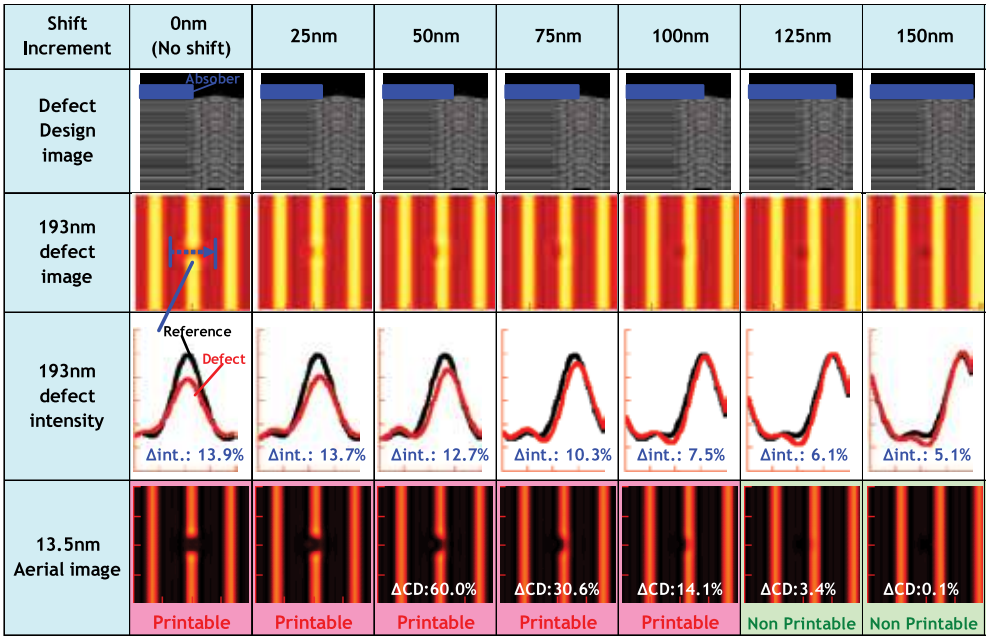

Figure 8. Defect intensity comparison at as the pattern is shifted relative to the defect.

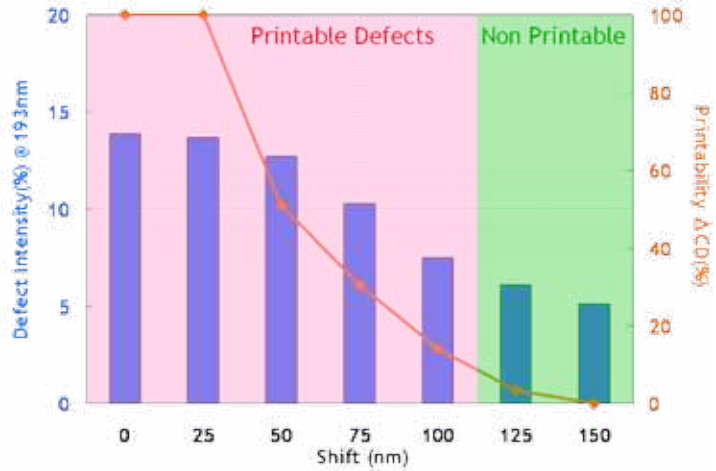

Figure 9. Defect intensity and printability as the defect shifts from the center of the clear area until it is completely buried under the absorber line.

Figure 6 shows the results of the smoothing study. In this case, the defect intensity is amplified slightly with the patterned absorber for most defect types and is supported by the results in Figure 4. Over all of the wavelengths studied, shorter wavelengths have larger near field defect intensities than longer ones. On the contrary, when studying perfect smoothing, longer wavelengths have higher near field defect intensities than shorter ones. The 488 nm wavelength shows the highest intensity with 532 nm and 365 nm following respectively. That result is consistent with the light penetration ranking shown in Figure 1. Unfortunately, none of these defect intensities is high enough for realistic detection. Since none of the non-actinic wavelengths can capture perfectly smoothed defects, we question whether smoothing should be deployed without actinic inspection. Smoothing will reduce printability at inspection wavelengths, but the defect will still have a printable impact at the EUV exposure wavelength.

2.1.4 Defect location study

Defect location relative to the mask absorber pattern is very important for both defect printability and for application to defect mitigation strategies[6] that shift the mask pattern relative to known defect locations. Figure 7 shows samples of the cases studied. The defect is a bump 5 nm high and

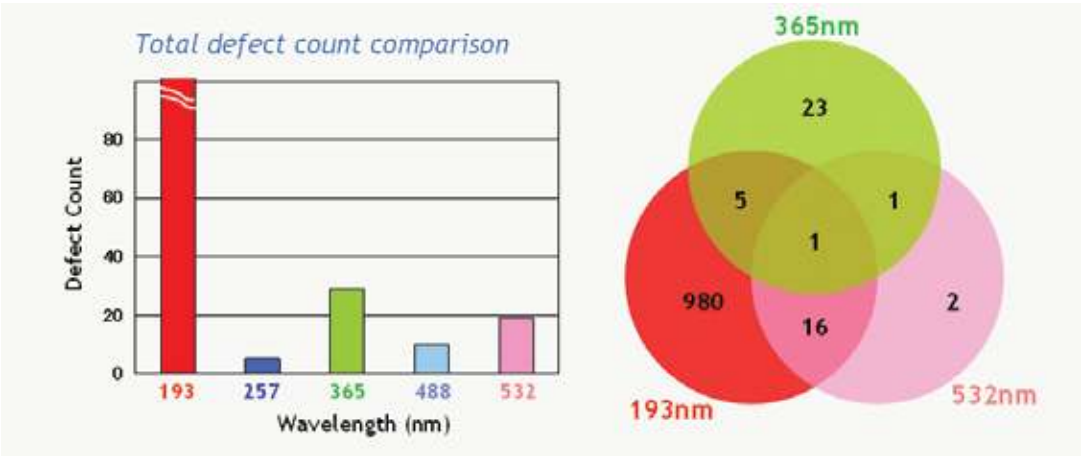

Figure 10. Native defect count is compared for various wavelength tools.

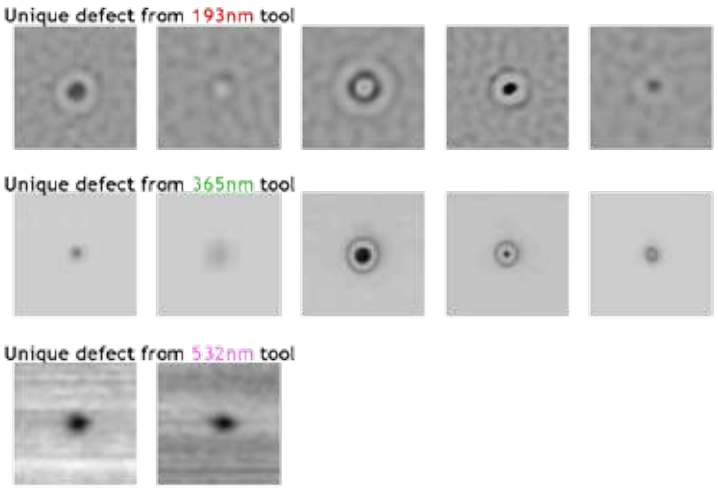

Figure 11. Examples of unique defect detections.

70 nm wide and is the defect signal is simulated as its location shifts in 25 nm increments from the center of a clear feature until it is completely covered by the absorber. The initial defect location, completely exposed in an etched area between two absorber images, is the no-shift case in Figure 7. The shift increments used in this study are 0, 25, 50, 75, 100, 125 and 150 nm.

Figure 8 shows the results from the defect location study. Both defect and reference intensities are calculated for each defect shift case at 193 nm exposure. Even for the150 nm shift case, where the defect is completely under absorber, differences can be seen between reference and defect intensities. This implies that all of these defects could be detectable, depending on the sensitivity threshold of the inspection tool. It was confirmed by simulating the same defect series at 13.5 nm, that the 125 nm and 150 nm shift defects are not printable.

Figure 9 shows the progression of 193 nm wavelength defect intensities as the pattern shifts relative to the defect. When the defect is centered on the clear area, the 193 nm wavelength defect intensity change is approximately 14%. This intensity decreases as the pattern shifts, ultimately ending at less than 6% with the defect completely under the absorber. Since the defects shifted by 125 nm and 150 nm were not printable, the 193 sensitivity to defects of this type appears to be sufficient. Of course, defect intensity and detectability will depend on many factors including the defect composition and physical dimensions.

2.2 Blank/Mask inspection

2.2.1 Blank inspection study

The EUV mask blank is composed of a 6” x 6” x 0.25” substrate coated with 20nm of CrN on the backside for electrostatic chucking and deposited with 40 to 50 alternating layers of Si and Mo on the front side for reflectivity. A thin Ru capping layer completes EUV blanks

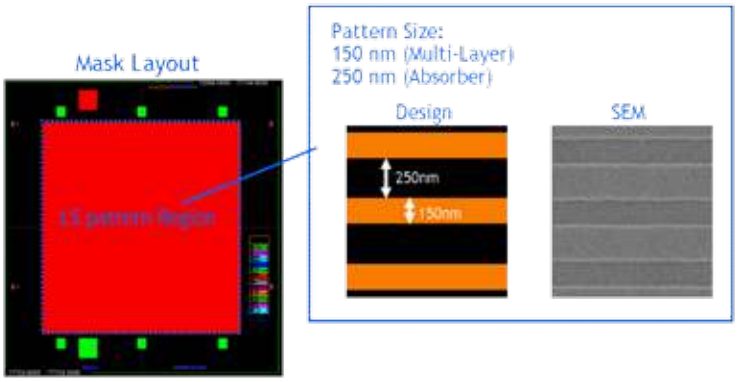

Figure 12. Test sample layout (left) and base pattern images (right).

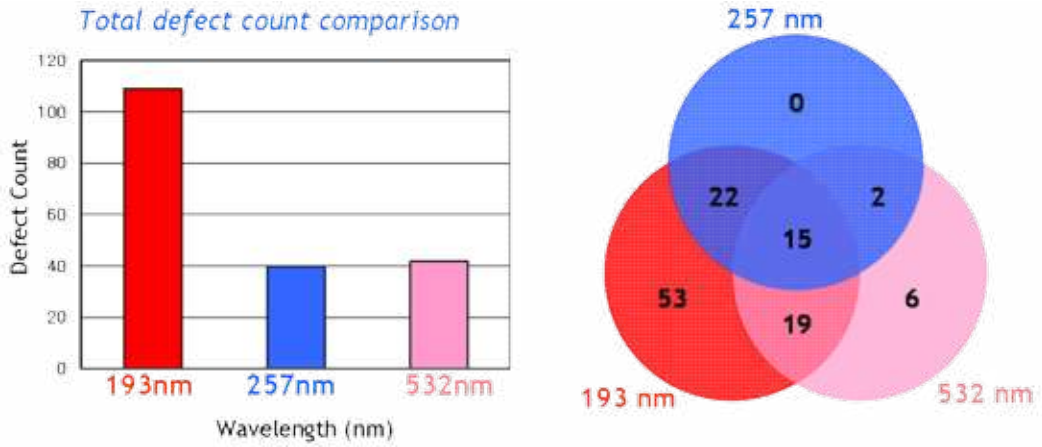

Figure 13. Defect counts obtained from three different wavelength tools are compared using a bar chart and a Venn diagram.

mirror surface to enhance durability. Inspection at this stage, before the absorber is deposited and creates an opaque layer on top of the mirror, is a critical point for quality assurance. We studied inspection results using the same set of wavelengths that were used in simulation: 193, 257, 365, 488 and 532 nm. The inspection results are summarized by total detected defects in Figure 10. The 193 nm tool demonstrated the highest sensitivity with 1002 defects detected, including 980 unique defects (i.e., detected only at 193 nm). Although 365 and 532 nm wavelength inspections detected fewer defects than the 193 nm tool, there were some unique defects detected only by those wavelengths.

Figure 11 provides images of the unique defects detected only by 193, 365 or 532 nm inspections. Additional SEM and AFM analysis is required to determine if these are actual phase defects, however the detectability of each is clearly wavelength dependent.

2.2.2 Pattern inspection study

A simple line/space pattern of 250 nm/150 nm (absorber/space) is shown in Figure 12 and is used for this study. In this case 193, 257, and 532 nm wavelength inspection tools were used to compare capabilities.

Figure 13 shows the patterned inspection results for the three different wavelengths. Although 193 nm again detected the largest number of defects, some defects were detected only at 532 nm wavelength. There were no unique 257 nm detections.

Figure 14 shows an example of a range of defect analysis options applied to one of the defects common to all three inspections. SEM and TEM images show that the absorber is deformed, creating a partial spherical shell or bump. This defect was probably created by the removal of a particle that was added during the blank absorber sputtering process. This defect is printable and all three tools were able to detect it. The 532 nm tool demonstrates the highest intensity signal.

Figure 15 shows another example of a defect common to all the inspections. This defect was classified as a multilayer pit defect, and was probably created by the removal of a particle embedded in the top multilayers, or by subsequent damage. Again, the 532 nm tool shows highest intensity to this defect type. The defect intensity signals behave quite

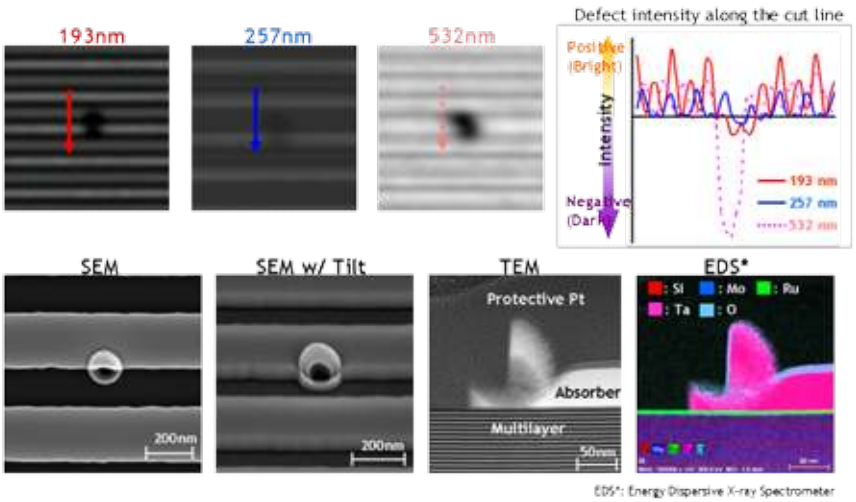

Figure 14. Defect images and intensity comparison (Example_1).

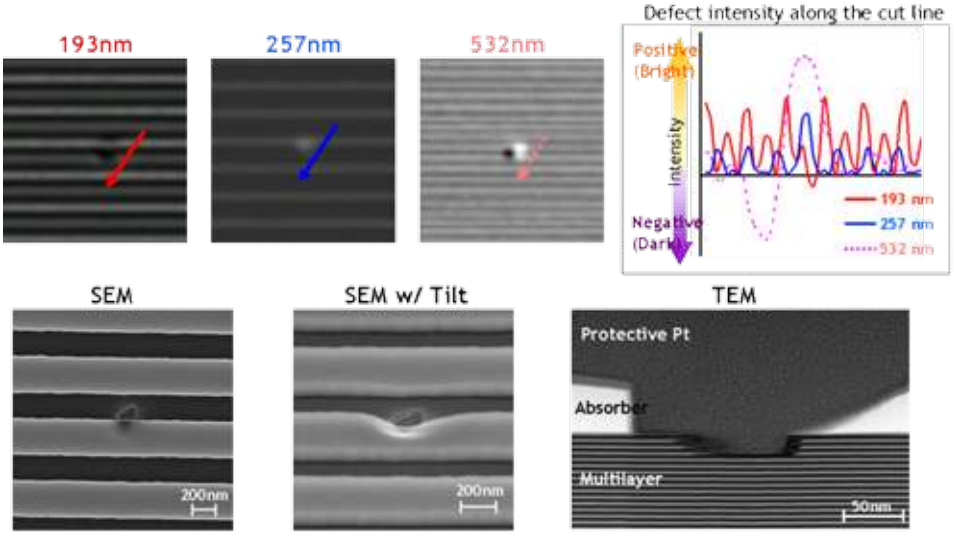

Figure 15. Defect image and intensity comparison (Example_2).

differently. Examining the cut line intensity curves, it is clear that the phase response differs. The 193 nm tool shows a slight negative (dark) intensity, the 257 nm tool shows a positive (bright) intensity and the 532 nm tool demonstrates both positive and negative intensity of a larger magnitude. These differences are anticipated since the detection systems are quite different; however the importance of the detection optics is underscored.

Figure 16 shows several unique defects that were detected only at the 193 nm wavelength. Most of them are amplitude defects such as particles and extensions. This result is expected since the 193 nm tool has higher resolution and imaging quality.

Figure 17 shows unique defect that was detected only by the 532 nm inspection tool. This defect looks similar to the defect shown in Figure 13 and is classified as an absorber defect. It was confirmed that this defect is a printable defect using AIT (*Actinic Inspection Tool*) microscope images. AIT images show bridged lines through focus.

Figure 18 shows one more example of a unique detection by the 532 nm tool. According to analysis results from the 13.5 nm wavelength AIT tool, ΔCD is 6.5% at best focus and 13.4% and 14.7% for negative and positive focus respectively. It is important to consider why the shorter wavelength tools could not detect this type of defect. One possibility is the wavelength dependence that has been discussed above. Another possibility is that light penetration is deeper for the longer wavelength as depicted in Figure 1. More detailed evaluations are needed to confirm. So far, this study suggests that a combination of wavelengths may

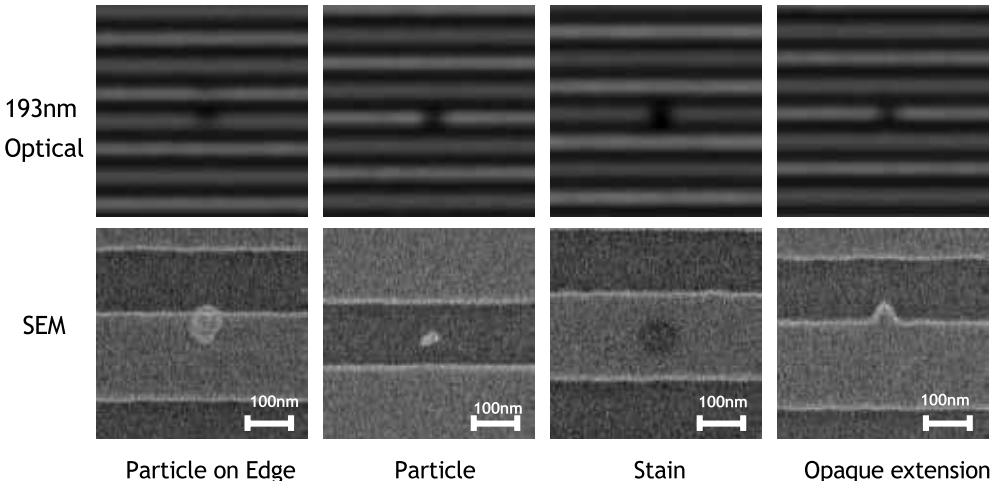

Figure 16. Examples of unique defects detected by 193 nm tool.

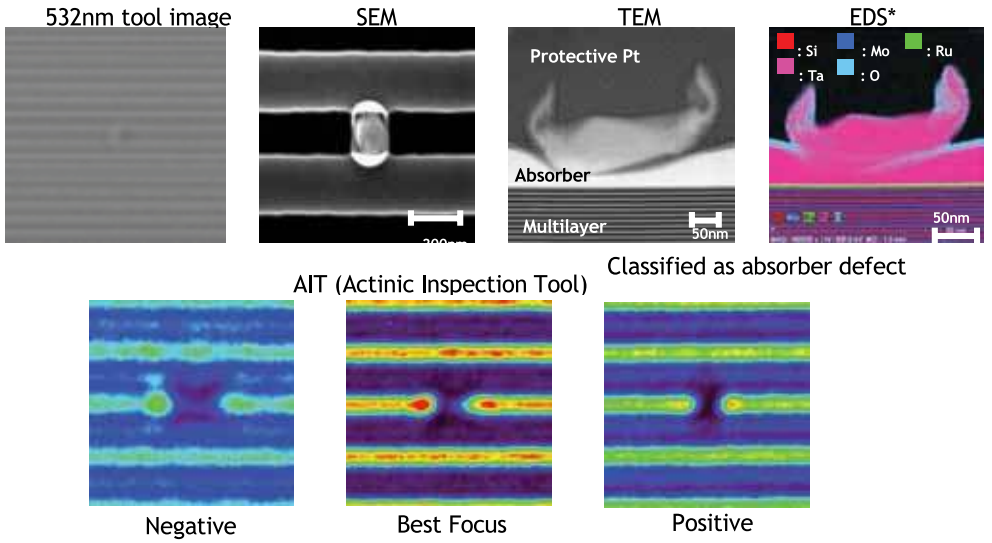

Figure 17. An example of a unique defects detected only by the 532 nm tool.

be the most comprehensive approach to finding printable defects as long as actinic inspection is not available.

3. Conclusions

3.1 Simulation study

A few conclusions can be drawn from this study. First, it was confirmed that longer wavelength light such as 532 nm, 488 nm, and 365 nm penetrate through more layers of Mo/Si than 193 nm light. Second, the data confirms that shorter wavelength light creates a larger near field defect intensity signal than longer wavelengths for most bump and pit defects. Additionally, it was observed that bumps tend to be slightly more detectable than pits, demonstrating roughly 10-15% larger intensity signals. In a smoothing case study, it was found that longer wavelengths can have higher defect intensity signals for some smoothing defects. Unfortunately, this enhanced intensity is too low for practical use. It was shown that smoothing in the multilayer deposition process has the potential to reduce inspection sensitivity while not impacting EUV printability, calling into question whether smoothing should be deployed without actinic inspection. Finally, in a study varying the placement of the phase defect relative to the absorber pattern, it was shown that non-actinic detectability follows a similar trend as EUV printability.

3.2 Blank and mask inspection study

The 193 nm inspection tool demonstrated higher sensitivity for both blank and pattern inspections in practice. It is important to note that despite lower total defect counts, the 365 nm, 488 nm and 532 nm wavelength tools detected

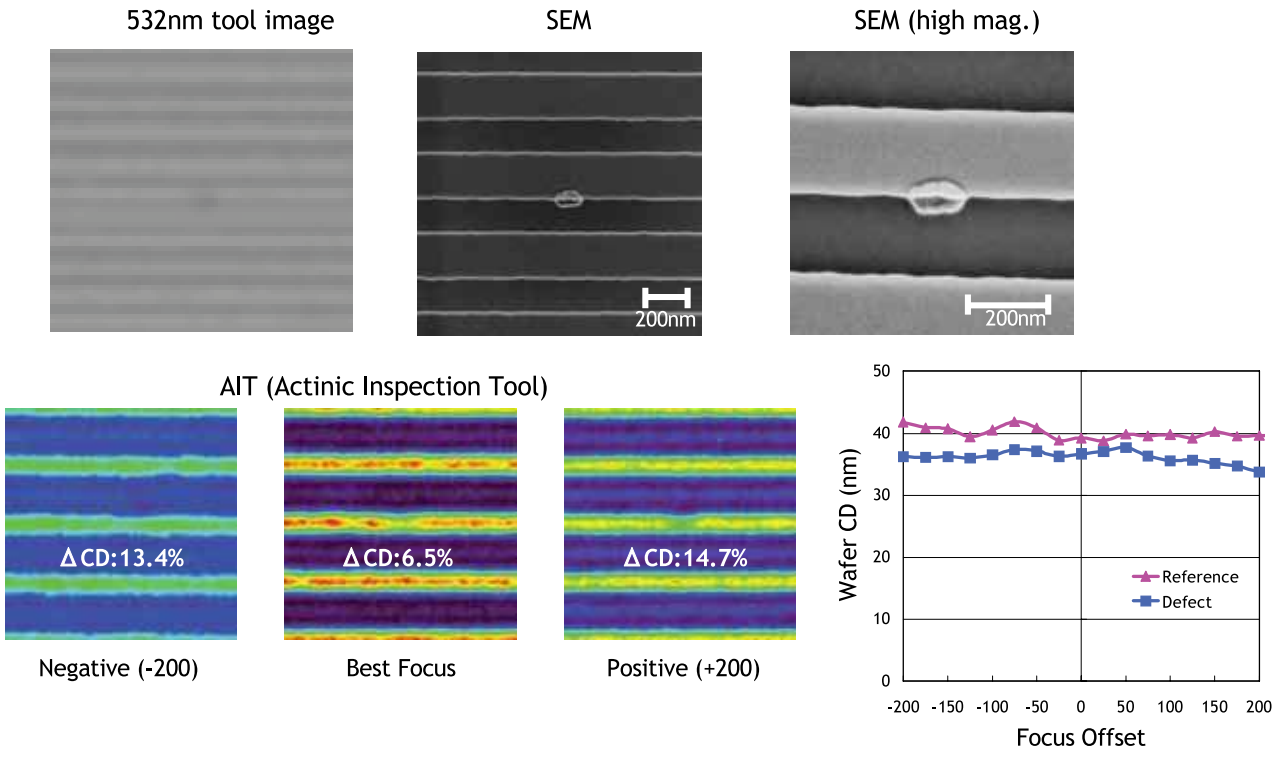

Figure 18. Example of a defect detected only by the 532 nm tool with AIT images and printability through focus.

some unique defects which were classified as printable defect by AIT analysis.

The overall conclusion is that the best way to assure EUV mask defect quality is to deploy a combination of 193 nm and longer wavelength inspections until actinic inspection tool is available. Further evaluation will be required to identify which of the longer wavelengths is most appropriate for both blank and pattern inspections.

4. Acknowledgments

The authors would like to thank Kenneth Goldberg of Lawrence Berkeley National Laboratory for AIT inspection and valuable guidance, Jenah Harris-Jones and John Underwood of SEMATECH for TEM work, the IBM/Toppan JDA team and IBM Mask House members for data collection and good discussions.

5. References

[1] "Defect inspection and repair performance comparisons between EUV and conventional masks", Kazunori Seki et al., **Proc. SPIE 7748**, 774807 (2010).

[2] "EUV mask: Ready or Not?", Emily Gallagher et al., International Symposia on EUV Lithography and Lithography Extensions (2011).

[3] "Defect Detection and Inspection Unmasked", Kenneth Goldberg, et al., International Workshop on EUV Lithography (2010).

[4] "Printability of native blank defects and programmed defects and their stack structures", Hyuk Joo Kwon et al., **Proc. SPIE 8166**, 81660H (2011).

[5] "The study of defect detection method for 32nm technology node and beyond", Kazunori Seki et al., **Proc. SPIE 7379**, 737928 (2009).

[6] "EUV mask defect mitigation through pattern placement", John Burns et al., **Proc. SPIE 7823**, 782340 (2011).

EDITORIAL *(continued from page 2)*

manufacturers. Open-content allows the manufacturers' development resources also to be leveraged, increasing the total number of ideas explored. Also, most windows of opportunity in the semiconductor industry are short if not sporadic, and new ideas usually arise as a solution for a current issue. Technological advancements may easily be missed if new ideas cannot be tested immediately. If the vendor is overloaded and cannot perform timely testing, a new idea – as worthy it may be – is already doomed. Open-content allows quick prototyping in that "what if we try this" moment without the road-block of unavailable capabilities or the delay of involving an external team.

Will increasing the number of open-content options cut into vendors' software-licensing fees? Unlikely...because total fees charged are not dictated by the number of fees nor the level of need for capabilities offered by the licensed software. Instead, the potential income of a vendor is dictated by the customers' return-on-investments (ROI). To justify higher investment fees paid by photomask-manufacturers, the equipment-vendor fees must enable a higher manufacturing return. If the end goal of utilizing new technology is to further reduce the cost of manufacturing while increasing product value, open-content is an ideal path to increased manufacturer ROI and vendor revenue.

How does this all tie into my earlier described after-work adventure? Both the USB-hubbed creation and photomasks are but the physical manifestations of an intangible collection of small ideas. The increased functionality of the stapler-sized file-server box was a direct result of "open-software" and "open-ideas" being built around an originally "closed" product. This same approach can be further applied to the world of photomask software – open thinking of small concepts leading to larger photomask advancements.

BACUS N • E • W • S

Sponsorship Opportunities

Sign up now for the best sponsorship opportunities

Photomask 2012 —
Contact: Lara Miles, Tel: +1 360 676 3290; laram@spie.org

Advanced Lithography 2013 —
Contact: Teresa Roles-Meier, Tel: +1 360 676 3290; teresar@spie.org

Advertise in the BACUS News!

The BACUS Newsletter is the premier publication serving the photomask industry. For information on how to advertise, contact:

Lara Miles
Tel: +1 360 676 3290
laram@spie.org

BACUS Corporate Members

FUJIFILM Electronic Materials U.S.A., Inc.
Gudeng Precision Industrial Co., Ltd.
HamaTech APE GmbH & Co. KG
Hitachi High Technologies America, Inc.
Ibss Group, Inc.
JEOL USA Inc.
KLA-Tencor Corp.
Max Levy Autograph, Inc.
Mentor Graphics Corp.
Mentor Graphics Corp.
Molecular Imprints, Inc.
Plasma-Therm LLC
Raytheon ELCAN Optical Technologies
XYALIS

Industry Briefs

Intel Invests in EUVL

By **Ned Stafford,** physicsworld.com

Intel has signed a major agreement with ASML to take a 15% stake for around €2.5bn and contribute €829m towards ASML's R&D in lithography-based IC manufacturing. ASML is developing a system for 450 mm wafers, doubling the capacity of chip-making factories at only a fraction of the cost. Brian Krzanich, Intel's COO, says the investment could result in 450 mm prototypes as early as 2015, noting that in the past transitions to bigger wafers have helped to cut costs by 30–40%. Intel's decision to invest in ASML should boost the near-term development of EUV technology, which some experts thought would not be ready for the next generation of chip-making technology. According to Intel officials, "Intel is saying it believes in this technology. It is really new but also really expensive. It is not something that a research institute could buy and use in the laboratory."

ASML says it is also in discussions with Samsung and the Taiwan Semiconductor Manufacturing Company about a stake in the firm. If those two companies agree to participate, their stakes combined with Intel's could total a 25% share of ASML.

Micropunching Lithography Could Yield Pliable Cell Phones and Laptops

By **Herb Booth,** UTA News Center

UT Arlington Professor Cheng Luo envisions the day that a flexible cell phone could be folded and placed in a pocket like a billfold or that a laptop computer could be rolled up and stored. Through a $300,000 National Science Foundation grant, the mechanical and aerospace engineering professor is developing a process called "micropunching lithography" to create lightweight, low-cost and flexible polymer-based devices. Practical applications for these microstructures could be in everything from glucose monitoring and delivery of chemicals in treating water pipes.

Micropunching lithography involves two operations: cutting and drawing. In these two operations, polymers are deformed using rigid and soft molds, respectively, creating desired polymer channels and sidewalls that can be used for detection and delivery. These novel microstructures of conducting polymers could be used as sensors and actuators for engineering and biomedical applications.

London Calling: Mirror, Mirror on the EUV Machine

By **Peter Clarke,** EETimes

The German Ministry of Education and Research (BMBF) is putting 7 million euro (about $8.5 million) towards a three-year project to improve the optics inside EUV lithography machines and help take resolution down to 14-nm and below. The project is led by Carl Zeiss SMT GmbH (Oberkochen, Germany), which is leading a team of seven German companies. If the money is spent right, it should help maintain Europe's lead in chip lithography. Carl Zeiss optical systems are already used in the EUV lithography machines produced by ASML (Veldhoven, The Netherlands).

The work will be on the illumination system and the projection optics. This includes mirror facets for an optical switching system and an innovative design for the surfaces of the reflection mirrors in the projection lens. Because the whole project is close to the limits of resolution, work will need to be done in the fields of optical measurement, micro-cooling and precision engineering.

Join the premier professional organization for mask makers and mask users!

About the BACUS Group

Founded in 1980 by a group of chrome blank users wanting a single voice to interact with suppliers, BACUS has grown to become the largest and most widely known forum for the exchange of technical information of interest to photomask and reticle makers. BACUS joined SPIE in January of 1991 to expand the exchange of information with mask makers around the world.

The group sponsors an informative monthly meeting and newsletter, BACUS News. The BACUS annual Photomask Technology Symposium covers photomask technology, photomask processes, lithography, materials and resists, phase shift masks, inspection and repair, metrology, and quality and manufacturing management.

Individual Membership Benefits include:

- Subscription to BACUS News (monthly)
- Complimentary Subscription *Semiconductor International* magazine
- Eligibility to hold office on BACUS Steering Committee

spie.org/bacushome

Corporate Membership Benefits include:

- Three Voting Members in the SPIE General Membership
- Subscription to BACUS News (monthly)
- One online SPIE Journal Subscription
- Listed as a Corporate Member in the BACUS Monthly Newsletter

spie.org/bacushome

Calendar

2012

SPIE Photomask Technology

11-13 September 2012
Monterey Marriott and
Monterey Conference Center
Monterey, California, USA
spie.org/pm

Late abstract submissions may be considered by the Chairs. Please send to Pat Wight at patw@spie.org.

2013

SPIE Advanced Lithography

24-28 February 2013
San Jose Convention Center and
San Jose Marriott
San Jose, California, USA
spie.org/al

SPIE Photomask Technology

10-12 September 2013
Monterey Marriott and
Monterey Conference Center
Monterey, California, USA

SPIE is the international society for optics and photonics, a not-for-profit organization founded in 1955 to advance light-based technologies. The Society serves nearly 225,000 constituents from approximately 150 countries, offering conferences, continuing education, books, journals, and a digital library in support of interdisciplinary information exchange, professional growth, and patent precedent. SPIE provided over $2.7 million in support of education and outreach programs in 2011.

SPIE

International Headquarters
P.O. Box 10, Bellingham, WA 98227-0010 USA
Tel: +1 360 676 3290
Fax: +1 360 647 1445
help@spie.org • SPIE.org

Shipping Address
1000 20th St., Bellingham, WA 98225-6705 USA

SPIE Europe
2 Alexandra Gate, Ffordd Pengam, Cardiff,
CF24 2SA, UK
Tel: +44 29 2089 4747
Fax: +44 29 2089 4750
spieeurope@spieeurope.org • www.spieeurope.org

You are invited to submit events of interest for this calendar. Please send to lindad@spie.org; alternatively, email or fax to SPIE.